



# Investigation of iron deficient and manganese doped Ni–Mg nano-ferroxide ceramics

Abhilash Pathania<sup>a,b</sup>, Preeti Thakur<sup>b</sup>, Amit Sharma<sup>c</sup>, J.H. Hsu<sup>d</sup>, Atul Thakur<sup>b,\*</sup>

<sup>a</sup>Department of Mechanical Engineering, Shoolini University, Solan, H.P. 173212, India

<sup>b</sup>Center of Excellence in Nanotechnology, Shoolini University, Solan, H.P. 173212, India

<sup>c</sup>Nanotechnology Wing, Innovative Science Research Society, Shimla H.P. 171002, India

<sup>d</sup>Physics Department, National Taiwan University, Taipei 106, Taiwan

Received 3 April 2015; received in revised form 5 May 2015; accepted 5 May 2015

Available online 14 May 2015

## Abstract

Mn substituted ferrite series  $\text{Ni}_{0.5-x}\text{Mn}_x\text{Mg}_{0.5}\text{Fe}_{1.98}\text{O}_4$  with  $x=0.0, 0.1, 0.2, 0.3, 0.4$  were prepared by a coprecipitation method. Samples were sintered at 600 °C for 3 h in a muffle furnace. Ferrite ceramics so obtained were characterized by X-ray diffraction (XRD), Scanning Electron Microscopy (SEM), Transmission Electron Microscopy (TEM), Fourier Transform Infrared Spectroscopy (FTIR) and Vibrating Sample Magnetometer (VSM) for their structural, morphological, optical and magnetic properties. XRD results confirmed cubic spinel structure with an average crystallite size in the range 33–47 nm. FTIR spectra showed the two main absorption bands in the range 400–600  $\text{cm}^{-1}$  arising due to tetrahedral and octahedral stretching vibrations. Saturation magnetization increases with  $\text{Mn}^{2+}$  ion content, attains a maximum value of 35.7 emu/g at  $x=0.2$  and then decreases. This can be attributed to super exchange interactions between cations in the spinel- lattice upon Mn substitution.

© 2015 Elsevier Ltd and Techna Group S.r.l. All rights reserved.

**Keywords:** C. Magnetic properties; Magnetic materials; Nanostructures; Chemical synthesis; X-ray diffraction

## 1. Introduction

Soft ferrites are important electronic materials for industry because of their good dielectric and magnetic properties [1]. Among soft ferrites, spinel ferrites have a wide range of applications in fields like electromagnetic devices, high density data storage, magnetic sensor, spintronics, magnetically guided drug delivery, magnetic resonance images etc. [2,3]. In order to achieve materials with desired physical and chemical properties, synthesis of these ferrites has become an essential focus of research and development activities. Various techniques to prepare spinel ferrites have been reported, e.g., citrate-precursor method [4], ball-milling technique [5], coprecipitation [6], polymeric assisted route [7], hydrothermal

method [8], reverse micelles process [9], and micro-emulsion method [10]. Chemical coprecipitation method has numerous advantages over other methods such as processing simplicity, reduced cost, less time consumption, high level of reactivity, narrow crystallite dispersion and homogenous mixing of the component materials [11]. Further, the properties of ferrites can be modified by substitution/addition of different dopants and also by controlling the sintering temperature or time [12]. Soft ferroxide based ceramics such as Mn–Zn, Ni–Zn, and Mg–Mn are well known ferrites covering a wide range of applications [13,14]. Bao et al. reported Mn substitution can lower the dielectric permittivity of  $\text{Co}_2\text{Z}$  hexagonal ferrite [15]. Bai et al. reported improvement in dielectric properties upon Mn substitution in Y-type hexagonal ferrite [16]. Dionne et al. proposed that  $\text{Mn}^{3+}$ , when present at certain concentrations, induces magnetostriction compensation and subsequently affects magnetic permeability [17]. Yue et al. reported that Mn substitution in NiCuZn ferrites remarkably affects the

\*Corresponding author. Tel.: +91 1792 654049.

E-mail addresses: [preetithakur@shooliniuniversity.com](mailto:preetithakur@shooliniuniversity.com) (P. Thakur), [atulphysics@gmail.com](mailto:atulphysics@gmail.com) (A. Thakur).

dependencies of magnetic and electric properties on frequency and temperature [18]. As per the literature survey, very little work has been reported on  $\text{Mn}^{2+}$  substituted Ni–Mg ferrites. Moreover, deficiency in iron and addition of manganese are helpful in suppressing the formation of  $\text{Fe}^{2+}$  ions and maintaining low loss [19]. Therefore, in the present study, Mn doped and iron deficient Ni–Mg nanoferrites have been prepared by a coprecipitation method and investigated for microstructural, optical and magnetic properties.

## 2. Experimental detail

Nanocrystalline spinel ferrites of general composition  $\text{Ni}_{0.5-x}\text{Mn}_x\text{Mg}_{0.5}\text{Fe}_{1.98}\text{O}_4$  with  $x=0.0, 0.1, 0.2, 0.3, 0.4$  were prepared by a coprecipitation method. Analytical grade nickel chloride (99.9% Merck, India), manganese chloride (99.5% Merck, India), magnesium chloride (99.9% Merck, India), and ferric chloride (99.5% Merck, India), were used in proper stoichiometric proportions. The base solution used was sodium hydroxide (NaOH). These chemicals were added to the boiling solution of NaOH (0.40 mol/l) under magnetic stirring to form a uniform mixture so that segregation of phases do not take place. Reaction was continued for 30 min at a temperature of 90 °C under vigorous stirring (~1000 rpm). Precipitates were separated and washed carefully with distilled water six times to remove the contents of impurities. Residues were dried in an electrical oven at 60 °C overnight, crushed manually for 5 min and then sintered at 600 °C for 3 h in a box type muffle furnace at a heating rate of 300 °C/h. X-ray diffraction (XRD) measurements were performed on a Philips PW 1729 Diffractometer using  $\text{CuK}\alpha$  radiation. Transmission Electron Microscopy (TEM) images were obtained from Jeol JEM-100CX. Field emission scanning electron micrographs (FE-SEM), energy dispersive X-ray spectroscopy (EDS) were recorded using MIRA3TESCAN SEM. PerkinElmer Spectroscopy was used to measure IR spectra. Magnetization curves were recorded on Vibrating Sample Magnetometer (VSM). All the measurements were performed at room temperature.

## 3. Results and discussion

XRD pattern of all the samples is shown in Fig. 1. All diffractograms showed the characteristic peaks corresponding to the planes (220), (311), (222), (400), (422), (511), and (440) which confirm the formation of cubic spinel phase, rejecting the presence of any other secondary phase formation. The line width analysis of diffraction patterns show considerable broadening, indicating nanometric behavior of the synthesized ferrite powder. Average crystallite size is calculated from the most prominent peak (311) by using Scherrer's formula [20]

$$D = \frac{0.9\lambda}{\beta \cos \theta} \quad (1)$$

where  $D$  is crystallite diameter, 0.9 is Scherrer's constant,  $\lambda$  is the X-ray wavelength corresponding to  $\text{CuK}\alpha$  ( $\lambda=1.5406 \text{ \AA}$ ),  $\beta$  denotes full-width at half-maximum of the peak, and  $\theta$  is Bragg's angle. The observed value is found to be

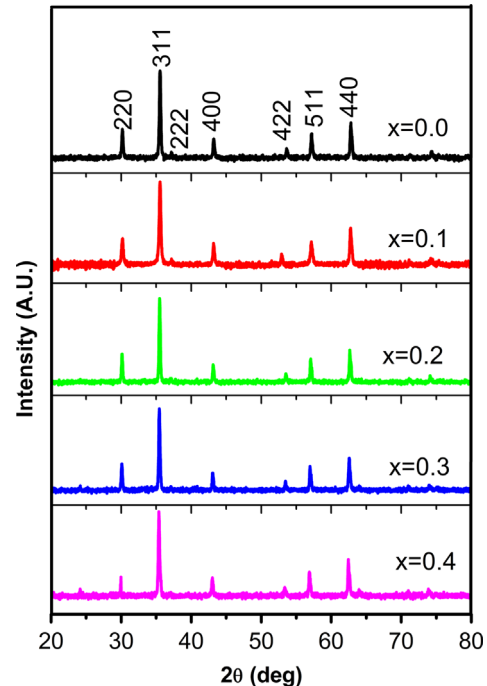


Fig. 1. XRD patterns for  $\text{Ni}_{0.5-x}\text{Mn}_x\text{Mg}_{0.5}\text{Fe}_{1.98}\text{O}_4$  samples.

in the range 33–47 nm which is lesser than the crystallite size (50–60 nm) reported by Hossain et al. [3]. Comparatively, smaller crystallite size may be due to iron deficiency created in the lattice. It is observed that with an increase in  $\text{Mn}^{2+}$  content, the crystallite size also increases. Lattice parameter ' $a$ ' is determined using the Bragg's law and the values are tabulated in Table 1. The lattice constant increases with increasing  $\text{Mn}^{2+}$  content in the series  $\text{Ni}_{0.5-x}\text{Mn}_x\text{Mg}_{0.5}\text{Fe}_{1.98}\text{O}_4$  obeying Vegard's law [21]. This increase can be attributed to the size difference of cations since the unit cell expands when the substituted cation size is larger. The ionic radius of  $\text{Mn}^{2+}$  (0.089 nm) is greater than that of  $\text{Ni}^{2+}$  (0.077 nm). Bulk density of the sintered samples was measured from mass and dimensions of the samples, whereas the theoretical density ( $\rho_x$ ) is calculated using the relation [22]

$$\rho_x = \frac{8M}{Na^3} \quad (2)$$

where  $M$  is molecular weight,  $N$  is Avogadro's number and ' $a$ ' is lattice parameter. The porosity of the samples is calculated using the relation

$$P = 1 - \frac{\rho_b}{\rho_x} \quad (3)$$

where  $\rho_b$  is the observed X-ray density. Table 1 indicates the theoretical density, observed density and porosity of different compositions. It is observed that porosity increases with an increase of  $\text{Mn}^{2+}$  substitution in Ni–Mg ferrites. Average lattice strain experienced by nanocrystallites is calculated from the Hall–Williamson plots using the relation [23]

$$\text{Average lattice strain (LS)} = \frac{\beta \cos \theta}{4 \sin \theta} \quad (4)$$

where  $\beta$  is integral breadth of the reflection located at  $2\theta$  (in

Download English Version:

<https://daneshyari.com/en/article/1460045>

Download Persian Version:

<https://daneshyari.com/article/1460045>

[Daneshyari.com](https://daneshyari.com)